research paper *Wader Study* 128(3): 226–237. doi:10.18194/ws.00250

Exploring the Dotterel Mountains: Improving the understanding of breeding habitat characteristics of an Arctic-breeding specialist bird

Christian Hoefs[1,2]*, Tim van der Meer[3], Peter Antkowiak[4], Jonas Hagge[5], Martin Green[6] & Jannis Gottwald[1]

[1]*Department of Geography, Philipps-University Marburg, Deutschhausstraße 12, 35037 Marburg, Germany*
[2]*Bioplan Marburg: Ecological Consultancy for Environmental Planning, Deutschhausstraße 36, 35037 Marburg, Germany*
[3]*Van der Goes en Groot Ecological Consultancy, Hazenkoog 35-A, 1822 BS Alkmaar, The Netherlands*
[4]*Department of Forestry Economics and Forest Planning Albert-Ludwigs-University, Freiburg, Germany*
[5]*Forest Nature Conservation, Georg-August-University, Büsgenweg 3, 37077 Göttingen, Germany*
[6]*Department of Biology, Biodiversity Unit, Lund University, Ecology Building, SE 223 62 Lund, Sweden*
**Corresponding author: christianhoefs@gmail.com*

Hoefs, C., T. van der Meer, P. Antkowiak, J. Hagge, M. Green & J. Gottwald. 2021. Exploring the Dotterel Mountains: Improving the understanding of breeding habitat characteristics of an Arctic-breeding specialist bird. *Wader Study* 128(3): 226–237.

Arctic-breeding birds are of particular conservation concern since their habitats are subject to severe changes and shifts upwards in both altitude and latitude due to global warming. Detailed knowledge on habitat characteristics of those species is required to understand how specialized Arctic-breeding species deal with changing habitat conditions. Therefore, sufficient data and methods to assess habitat suitability on large spatial scales in a time- and cost-efficient way are needed. The Eurasian Dotterel *Charadrius morinellus* is a specialist high altitude and Arctic-breeding wader and can serve as an ideal model species for addressing habitat requirements of Arctic-breeding birds and consequences for conservation. We combined field surveys with remote sensing data to develop a distribution model for the breeding habitat of the Eurasian Dotterel in the Vindelfjällen Nature Reserve in northern Sweden. The remote sensing data comprised 211 spectral, structural and topographic indices derived from freely available satellite images and digital elevation models. For species distribution modeling we used MaxEnt with an advanced variable and parameter selection method for model training. The trained model produced excellent results (AUC = 0.99) with seven resulting predictor variables reflecting the habitat requirements of the Dotterel: sparsely vegetated mountain tops with dry ground which are very open. This study further highlights the potential of combining survey data with freely available remote sensing data for detailed area-wide population predictions and the monitoring of habitat change as a tool in species conservation.

Keywords

Eurasian Dotterel

modeling

Arctic

remote sensing

prediction

species distribution modeling

INTRODUCTION

Arctic ecosystems are subject to severe habitat changes and are the most vulnerable to global warming (Virkkala *et al.* 2014). The Arctic tundra has already experienced vast changes within the last few decades and faces rapid shifts in habitat and species composition, both in altitude and latitude (Chen *et al.* 2011, Engler *et al.* 2013, Lindström *et al.* 2013, Steinbauer *et al.* 2018), possibly leading to the extinction of many species (Urban 2015). At the same time, Arctic-tundra ecosystems are important breeding grounds for many migratory bird species, particularly waders (Wauchope *et al.* 2016). They benefit from low numbers of predators and exploit the Arctic summers' temporarily available food resources to raise their offspring (Tulp & Schekkerman 2008, Lindström *et al.* 2013, 2015, Saalfeld *et al.* 2013). Species breeding in high altitude- and latitude-habitats are particularly sensitive to environmental changes since the species co-evolved to suit their environmental conditions, which are now changing faster than they can evolve (Hof *et al.* 2016, Scridel *et al.* 2018). Wauchope *et al.* (2016) showed that 66–83% of Arctic-breeding wader species will lose the majority of

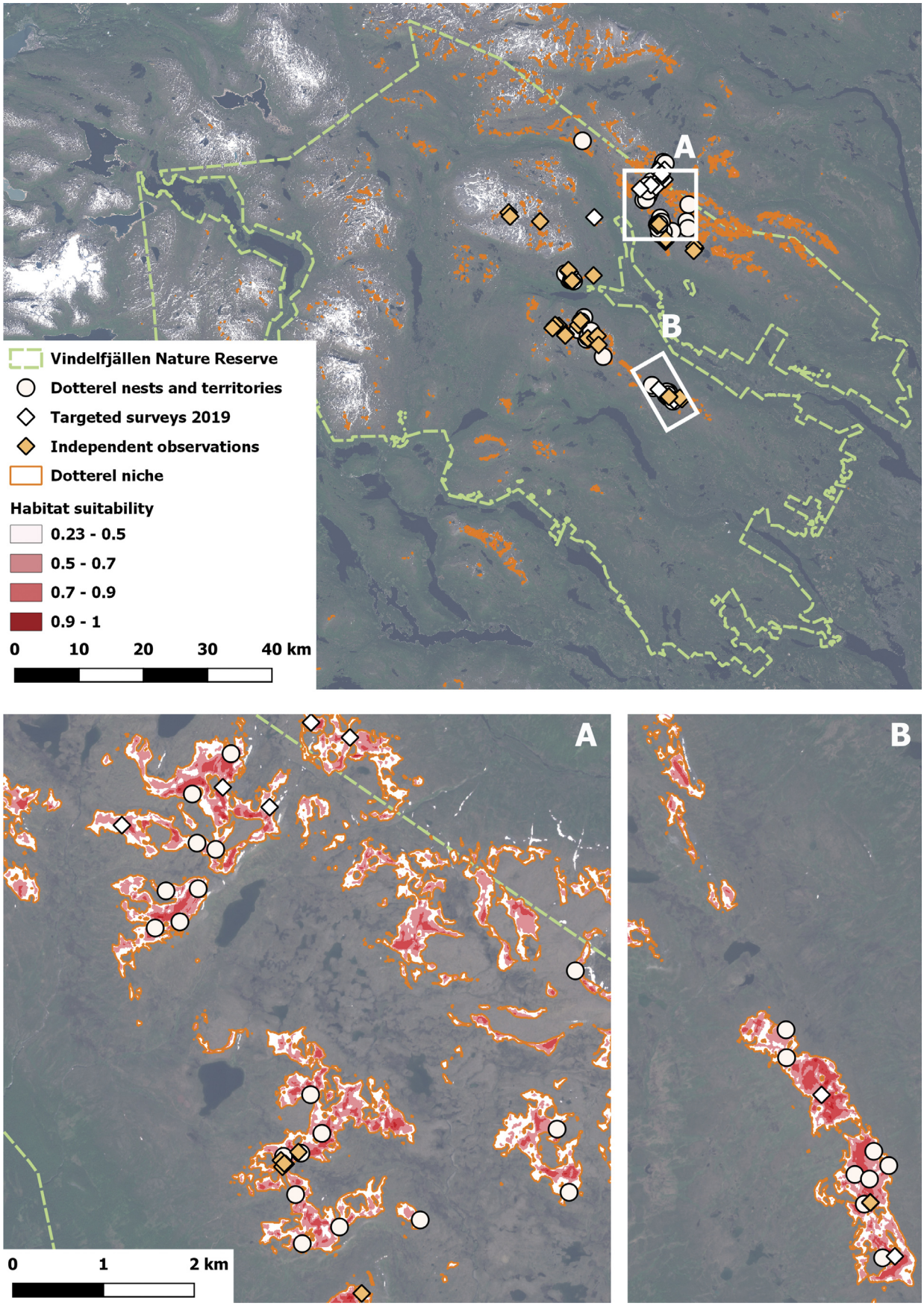

Fig. 1. Map showing the Vindelfjällen Nature Reserve with main study areas (A = Björkfjället, B = Kraipe), Dotterel nests and territories from 2016–2018 as well as independent observations (see *Methods*) and targeted surveys from 2019. Area of predicted suitable Dotterel breeding habitat according to our MaxEnt model, dropping the lowest 10th percentile with habitat suitability values >0.23 for niche delineation. Habitat suitability is given in four classes. Image source: Sentinel-2A satellite data (*https://scihub.copernicus.eu*) sampled on 2 Jul 2018.

their present suitable breeding habitat within the next 70 years, exceeding the impact of the Mid-Holocene climatic optimum. Several studies on Arctic-breeding shorebirds have reported contraction of breeding range and declines in population size (Scridel *et al.* 2017, Lehikoinen *et al.* 2018, Ewing *et al.* 2020). Simultaneously, the ranges of generalist species and particularly predators are migrating further poleward, which increases competition for breeding habitat and predation pressure for specialized Arctic species (Callaghan *et al.* 2011).

Gaining knowledge on how species may deal with changing habitat conditions requires detailed information of species habitat associations as a foundation for predicting their vulnerability. In addition, identifying areas with suitable habitat conditions is key to successful conservation planning (Saalfeld *et al.* 2013). Species breeding on the Arctic tundra often have vast distribution ranges in remote, largely inaccessible areas, resulting in limited applicability of commonly used census methods. Therefore, identifying a cost- and time-efficient method that is capable of identifying areas with suitable habitat conditions on large spatial scales is vital for the protection of these specialist species.

Combining high-resolution remote sensing data with powerful machine-learning algorithms has great potential to serve as a tool for predicting area-wide species distributions over large spatial scales (Lathrop *et al.* 2018, Leitão & Santos 2019). Taking advantage of the regular acquisition of satellite images enables us to predict and monitor habitat availability, changes and shifts by applying fitted models in subsequent years. Using limited presence-only data combined with a variety of remote sensing-derived predictor variables has proven to be an efficient method to predict species distributions (Kerr & Ostrovsky 2003, Leitão & Santos 2019). Maximum entropy (MaxEnt) modeling (Phillips *et al.* 2006) offers the opportunity to predict species distribution by presence-only data.

Here, we applied a workflow that uses MaxEnt to predict the present breeding distribution of an Arctic specialist bird, the Eurasian Dotterel *Charadrius morinellus* (hereafter Dotterel) in the Vindelfjällen Nature Reserve in northern Sweden. The Dotterel serves as an ideal species to use for MaxEnt modeling as it is highly specialized to a narrow ecological niche. It also suffers from severe population declines at the edge of its range in the UK, where distribution shifts both geographically northwards and upwards in elevation are being observed (Huntley 2007, Eaton *et al.* 2015, Hayhow *et al.* 2015, Baxter 2016, Ewing *et al.* 2020). The decline of species at their distribution edges is known to indicate an overall decline in species populations (Hampe & Petit 2005, Vilà-Cabrera *et al.* 2019). According to Huntley (2007), the Dotterel will lose the majority of its present European breeding distribution by the end of the 21st century.

We used our field data with Dotterel territories and nests from 2016, 2017 and 2018 as presence-only data for the modeling process. In this study, we aim to (1) define the most predictive remote sensing, data-derived variables and (2) give an accurate potential present distribution for the species within our study area, which is representative of Arctic ecosystems with associated breeding birds (Staafjord 2012, Svensson & Andersson 2013). The performance of the model was validated by targeted surveys in areas with well-predicted habitat quality and independent field data provided by the Swedish bird-monitoring scheme.

Establishing a large-scale habitat model, derived from limited field data (site occupancy of birds) and freely available remote sensing data enables the identification of areas of high conservation value for Dotterel. Our model will also allow us to monitor climate change-induced habitat loss by repeatedly applying it on regularly acquired satellite images in subsequent years. It will further allow us to extrapolate a population size estimation with detailed species habitat associations.

METHODS

Study area

The Vindelfjällen Nature Reserve (hereafter Vindelfjällen) is located in Swedish Lapland south of the Arctic Circle and close to the border with Norway (65.95°N, 16.20°E). It surrounds the village of Ammarnäs and covers an area of 5,500 km² (Fig. 1). It is one of the largest protected areas in Sweden and comprises an elevation gradient from 500 m to 1,768 m asl with taiga forests in the valleys (coniferous and birch forests) and different types of Arctic tundra at higher elevations. The treeline is at ~800 m asl (Staafjord 2012). The reserve is designated as an Important Bird Area (IBA) and Special Protected Area (SPA) for birds under the European Union's Birds Directive (BirdLife International 2019). The main tundra habitats can be differentiated into four types: dry heathland, willow scrub, wet areas and alpine meadows (Svensson & Andersson 2013). Targeted bird surveys have been carried out in all major habitats in Vindelfjällen annually since 1963 as part of the LUVRE project and the Swedish Bird Survey (*https://www.luvre.lu.se/*). Dotterels mainly occur within the higher parts of the reserve mostly comprising of alpine meadows. While Dotterel populations are declining in the UK (Hayhow *et al.* 2015, Ewing *et al.* 2020) their breeding numbers have been relatively stable both in Fennoscandia (Lindström *et al.* 2019) and Vindelfjällen (Svensson & Andersson 2013, own unpubl. data). Because of this, the Dotterel breeding population in Vindelfjällen is particularly suitable for this study. We limited our main study sites to two areas (Björkfjället and Kraipe; see Fig. 1) that together host approximately 30 breeding pairs of Dotterels.

Study species

The Dotterel is a medium-sized, long-distance migratory wader that breeds in Arctic-alpine tundra ranging from Scotland through Siberia to western Alaska with disjunct distributions in mountain ranges like the Alps (BirdLife International 2021).The alpine breeding habitat is characterized by open, sparsely vegetated mountain plateaus and ridges with short grasses, mosses and lichen, with a

Fig. 2. Breeding Dotterel male in typical habitat with a composition of bare ground, short vegetation, moss cover and rocks (photo: Christian Hoefs).

high proportion of bare ground, rocks and rocky debris (Fig. 2; Marchant *et al.* 1986, Galbraith *et al.* 1993, Whitfield 2002, Baxter 2016, Gejl 2017).

Presence data: Dotterel surveys

The two study areas within Vindelfjällen (*ca.* 10 km²; see Fig. 1) were intensively surveyed for territorial and breeding Dotterels for three consecutive years (2016–2018). Both areas were visited 3–5 times per season, each visit comprising a full field day. The areas were surveyed by 3–6 persons, systematically walking in line 10–30 m apart, regularly scanning with binoculars for displaying birds or birds showing any breeding behavior (e.g. agonistic behavior, courtship behavior, distraction display, male and female feeding together). Only sightings of birds showing territorial or breeding behavior on the ground during the breeding season were included in the model – aerial displays were not included. Sampling effort was not necessarily consistent across seasons or years, but we consider this to have a negligible impact on our modeling approach due to its robustness towards variable sampling effort (see below). We found 23 Dotterel nests and 156 locations with territories. Since the Dotterel is a highly specialized species, we assume that territory locations have similar habitat characteristics to nest locations. During fieldwork we regularly found nests within meters of where Dotterels were observed displaying on the ground. For these reasons, we used both territories and nests in the analysis and treated both as presence points. Territories less than 300 m apart were excluded from the analyses to minimize spatial autocorrelation and biasing the model by overrepresenting habitat preferences of birds in more intensively surveyed areas. We also deleted territorial points that were close (≤300 m) to nests from the same season to ensure independence between presence points. As the closest proximity of two nests in the same study area was less than 100 m, we chose the 300 m threshold to safely exclude pseudoreplicates of the same territorial pair. The final model was based on 48 presence points (23 nests and 25 territories).

Environmental data

Environmental data derived from remote sensing are frequently used in species distribution modelling (e.g. Saalfeld *et al.* 2013, Gottwald *et al.* 2017, Montenegro *et al.* 2017) and provide the advantage of allowing area-wide predictions of habitat suitability for studied species. Here, satellite data and Digital Elevation Models (DEM) provide the opportunity to calculate multiple measures of environmental characteristics (Lathrop *et al.* 2018).

In this study we used Sentinel-2A satellite data (*https://scihub.copernicus.eu/*) sampled on 2 July 2018. We chose this date as it was the closest available dataset to the typical hatching date of Dotterel in the area and therefore is representative of the chick-rearing period. Insect availability (as a food source for chicks) is closely related to snow cover, vegetation patterns and phenology (Høye & Forchhammer 2008, Tulp & Schekkerman 2008). Moreover, the image from 2018 was chosen because it represents an average snow cover for this time of year. We calculated a comprehensive dataset of vegetation indices that have

been found useful for vegetation mapping (Baugh & Groeneveld 2006, Puletti *et al.* 2017), based on formulae for Sentinel 2A products provided by the IndexDataBase (*https://www.indexdatabase.de/db/is.php?sensor_id=96*).

In addition, we calculated a set of texture metrics (TM; Haralick *et al.* 1973) in a grey level co-occurrence matrix (GLCM), which hold further, valuable information for classifications (Lu *et al.* 2014, Kupidura 2019). These grey level textures particularly show similarities or differences in contrast, coarseness and patterns that are not necessarily represented by vegetation indices. They have proven to be especially useful as measures for local heterogeneity of vegetation patterns within land cover classes (Lu *et al.* 2014, Kupidura 2019).

Furthermore, we used a digital elevation model (European Digital Elevation Model: EU-DEM v.1.1) to calculate topographic variables: slope, aspect, curvature, the Morphometric Protection Index, the Topographic Position Index and the Topographic Wetness Index with the SAGA-GIS morphometry toolset (Conrad *et al.* 2015, Watkins 2015). The final set of potential predictor variables for further modelling comprised 211 variables (42 spectral indices, 154 texture metrics and 15 topographic indices) in 10 m resolution.

Modelling breeding habitat suitability for the Dotterel using MaxEnt

We used MaxEnt (Phillips *et al.* 2006) for modelling distribution of Dotterel breeding habitat. MaxEnt modeling offers the opportunity to predict species distribution based on presence-only data by complementing these data points with a set of randomly selected background data points and is capable of handling many predictor variables (Phillips *et al.* 2006). Philipps & Dudik (2016) revealed that the performance of MaxEnt models increases with increasing background samples until it reaches a plateau at 8,000 samples.

To represent the environmental conditions of potentially unsuitable habitats in the modeling procedure, we followed the recommendations of Philipps & Dudik (2008) and generated 8,000 background samples randomly distributed over the entire Nature Reserve. MaxEnt is very robust even with small datasets (Phillips *et al.* 2006) and variation in sampling effort, as long as the minimum distance between presence points is set to a coarser scale than predictor variables (Fourcade *et al.* 2014). We meet this condition with the chosen 300 m minimum distance between presence points.

MaxEnt has two main parameters that can be manipulated to increase or decrease the complexity of models: regularization multiplier and feature classes. The regularization multiplier (beta-multiplier) is a positive numerical value that regulates how closely the resulting model will fit to the training data, with smaller values leading to a closer fit. The six feature classes provided in MaxEnt are mathematical transformations of the environmental variables used in the model to allow complex relationships beyond linear regressions to be modeled (Merow *et al.* 2013). Default settings of feature classes and the regularization multiplier are based on experimental assessments of the model performance over 226 species from six regions (Phillips & Dudík 2008) but are not necessarily valid for other studies. Morales *et al.* (2017) showed that most publications used MaxEnt's default settings without further testing of parameter configurations, which potentially leads to non-optimal and sometimes overly optimistic results.

Besides internal MaxEnt parameters, selecting the best combination of uncorrelated predictor variables is a key problem in predictive modeling. In species distribution modeling (SDM) it is often addressed by pre-selecting environmental variables based on expert knowledge about the biology of the target species (Leitão & Santos 2019). However, this approach often leads to suboptimal or even misleading model results compared to feature selection procedures that filter a subset of uncorrelated and highly contributing variables from a bigger set of potentially predictive candidate features based on reiterative performance tests (Warren & Seifert 2011, Zeng *et al.* 2016, Meyer *et al.* 2018).

To select the best performing model for our case study we tested all potential combinations of feature classes, and included predictor variables using a recursive feature selection procedure that accounted for variable correlation (Gottwald *et al.* 2017). Therefore, we calculated an initial model where all variables with a model contribution below 2% were excluded from further analysis. In the next step, the best performing variable was identified and all variables that correlated higher than $r = 0.7$ with that variable were removed. To assess the performance of the model as well as each individual variable, a 10-fold cross validation was performed using 50% of the presence data as the training sample. The model performance was then estimated on the remaining test data sample by the area under the curve (AUC) and the corrected Akaike Information Criterion (AICc; Warren & Seifert 2011). With the remaining set of variables, a new MaxEnt model was calculated. Variables with low contribution scores and remaining variables that were correlated to the variable of second-highest contribution were excluded. This process was repeated until a set of uncorrelated and highly contributing variables was left. Regularization multipliers between 0.5 (potential of over-fitting) and 3 (potential of over-generalization) with increments of 0.5 were tested for each combination of feature classes and predictors to avoid potential over-fitting at too small multiplier values and over-generalizations at too high values.

For the final model, we selected the one, which (1) considered fewer parameters than observation samples to avoid over-fitting, (2) showed the lowest AICc compared to models with equal parameter configurations and (3) had the highest average AUC on testing data among models selected based on lower AICc values.

To control for the robustness of the selected predictor variables we calculated the mean of their contribution over all 19,330 model runs. To verify the applicability of the habitat suitability prediction, we conducted targeted

surveys in areas predicted as suitable Dotterel habitat, in proximity to our regular field work areas in June 2019. To measure the predictive skill of the model we used independent field data of 47 occurrence locations from surveys conducted by Martin Green and Sophie Ehnbom (Swedish Bird Survey) as part of the annual survey routes in Vindelfjällen which were conducted within the study sites. These observations were used to calculate the AUC value and the continuous Boyce index with the R packages *dismo* and *ecospat,* respectively (Di Cola *et al.* 2017, Hijmans *et al.* 2021). The Boyce index is a threshold-independent evaluator for SDM predictions (Hirzel *et al.* 2006, Di Cola *et al.* 2017), which considers random model performance and only requires presences, likely making it the most appropriate metric in the case of presence-only models. Values vary between –1 and +1 with positive values indicating a model in which predictions are consistent with the distribution of presences, values close to zero indicating a random model and negative values indicating counter predictions (Hirzel *et al.* 2006).

MaxEnt produces probability maps of species presence (scales of 0–1 or 0–100). However, in many applications, binary maps (0/1) are required. Therefore, a minimum probability threshold has to be identified, that divides the distribution into presence and absence. In a study with 40 endemic mammals Escalante *et al.* (2013) showed that the 10th percentile of training presence was best suited for niche delineation. To define the spatial extent of potential Dotterel habitat we dropped all raster cells lower than the 10th percentile of the habitat suitability prediction values at training presence.

All analyses and visualizations were performed with the open source software packages R (R Core Team 2020) and QGIS (QGIS Development Team 2021).

RESULTS

The best performing MaxEnt model for the Dotterel breeding habitat suitability was selected from 19,330 models fitted using all potential combinations of feature classes and the applied multiplier range. It reached an overall test AUC of 0.998 based on a 10-fold cross-validation with 50% test data and included the MaxEnt feature classes *hinge*, *threshold, product* and *quadratic* with 0.5 as beta-multiplier. Whilst the feature class *threshold* has been omitted from the default feature classes selection in the recent version of MaxEnt (Phillips *et al.* 2017), the feature class *linear* was excluded in our case study. Instead of a beta-multiplier of 1, which is the default value in former and recent MaxEnt versions, our model selection procedure identified a beta-multiplier of 0.5 as the best performing value. The best performance was achieved based on a small subset of seven out of 211 initially provided environmental variables. Within the variable selection process, three spectral indices, two texture metrics and two topographic indices were selected as best performing predictor variables (Table 1). *Redness Index 200 m mean* and *Sentinel band 8 TM difference variance sd 200 m* showed the highest explanatory power (both 27.1%), followed by *Chlorophyll Vegetation Index 200 m mean* (24%), *Sentinel band 4 200 m mean* (8.5%), *Topographic Wetness Index* (5.4%), *Sentinel band 3 TM difference variance 200 m mean* (4.1%) and *Morphometric Protection Index 2,000 m* (3.8%; see Table 1).

With a mean AUC test of 0.98 and a standard deviation of 0.0016 over all models with a minimum AICc within the specific feature class settings, model results seem highly robust. The three best performing variables for the selected model had the highest mean contribution over all 19,330 model runs as well (*Redness Index 200 m mean* = 26%, *Chlorophyll Vegetation Index 200 m mean* = 13.7%, *Sentinel band 8 TM difference variance sd 200 m* = 13.6%). All other selected variables were among the 10% of best performing variables over all 19,330 model runs.

The response curves (Fig. 3) show the relation of each variable's contribution to the model with the respective probability of presence for the species. *Chlorophyll Vegetation Index* reached the highest probability of presence with values between 2.5 and 3 indicating a high chlorophyll content. *Morphometric Protection* and *Topographic Wetness Index* achieved highest probabilities for suitable Dotterel habitat with low values, gradually decreasing with increasing values. This indicates a high openness of the surroundings and relatively dry ground (see Table 1, Fig. 1 and *Discussion*) The *Redness Index* was most important at values ranging between –0.05 and 0.05. Texture Metrics (TM) for *Sentinel band 3 Difference Variance 200 m mean* had the highest probability with values between –0.25 and –0.05. *Sentinel band 4 200 m mean* had two peaks with values around 800 and 1,500. *Sentinel band 8 TM Difference Variance 200 m sd* gained a higher probability of presence with increasing values from 0.12, reaching a plateau at 0.23 until 0.26.

Performance measures showed excellent results, on both repetitively sampled 50% testing data from our field dataset used in the model selection procedure and the independent survey data that was not involved in the model selection procedure. The model gains further reliability through validation with the independent test data (see *Methods*) with AUC = 0.993 as well as a Boyce-Index = 0.863, which are both close to their potential maximum.

The resulting habitat suitability values of the MaxEnt model ranged between >0.001 and 0.991 with a mean value of 0.004 ± 0.035. The spatial visualization of habitat suitability, with survey points and independent observations are presented in four classes in Fig. 1. The threshold value for the Dotterel's niche delineation (see *Methods*) from habitat suitability values was 0.23, by dropping the lowest 10th percentile of values (Fig. 1). During our target surveys, we found eleven new territories and one nest within the predicted areas. Of 47 independent data points, 43 were inside our delineated niche. The remaining four points were between 25 m and 500 m outside our predicted niche.

The entire area with suitable Dotterel habitat within the Vindelfjällen Nature Reserve following our niche delineation

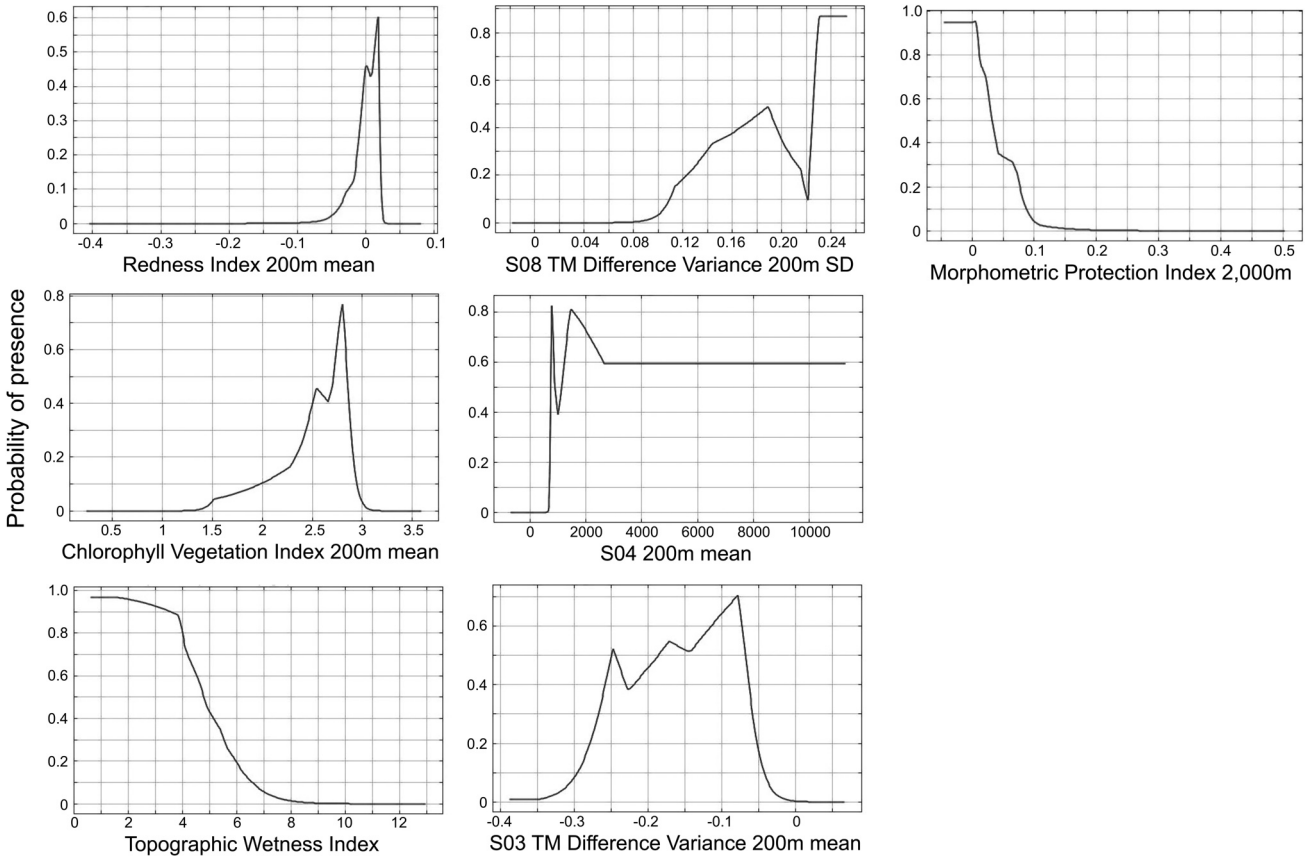

Fig. 3. Response curves for each variable used in the MaxEnt model showing the probability of presence of each variable depending on its value.

comprises 59.2 km², which is *ca.* 1.1% of the area of the Nature Reserve. With approximately 30 pairs (own unpubl. data) within the delineated niche area that we have surveyed well (*ca.* 10 km²), the breeding population of Dotterels in the entire Nature Reserve can be roughly extrapolated to approximately 180 pairs, given equal distribution over the predicted suitable breeding habitats.

DISCUSSION

Model performance

The model based on the seven remote sensing-derived predictor variables achieved a very high performance and seemed to hold important information serving as proxies for the Dotterel breeding niche´s ecological features. Parameter configurations of the best performing model differ from MaxEnt's former (Phillips & Dudík 2008) as well as recently adjusted (Phillips *et al.* 2017) default settings. Additionally, the best performing model was achieved based on a small subset of seven out of 211 initially provided environmental variables. The variable selection process for the model chose variables such as texture metrics whose interpretation is not straightforward. Therefore, their inclusion might not have been considered based on expert knowledge only. Some obvious variables missing in the model were either neglected in the variable selection due to negligible contribution or because of correlation with other variables. For example, *altitude*, *slope* and *exposure* are variables that are commonly used in SDMs, but seem to be outperformed by the set of indices that were used in our model. These findings confirm the necessity of the implementation of sophisticated parameter and variable selection procedures to obtain the best model results.

Implications of modelling suitable breeding habitat of Dotterels

Our results show that MaxEnt is capable of predicting the distribution patterns for the ecological niche of the Dotterel inhabiting the alpine ridges of the Arctic tundra in our study area. With seven remote sensing-derived predictor variables, we successfully predicted an area-wide habitat distribution in a representative spatial context with a high resolution (10 x 10 m).

The *Chlorophyll Vegetation Index* uses a near infrared by green band reflectance ratio to measure leaf chlorophyll concentration and combines this with a correction factor for varying vegetation cover or density (Vincini *et al.* 2008). It is therefore predictive of sparse or patchy vegetation as it occurs in preferred Dotterel habitat (Galbraith *et al.* 1993). The index had a major contribution to the model with values between 2.5 and 3.5, which corresponds

Table 1. Selected variables in the best performing MaxEnt model to predict breeding habitat suitability of the Dotterel. Formulae were taken from the IndexDataBase IDB (*https://www.indexdatabase.de/db/is.php?sensor_id=96*). S indicates the respective Sentinel-2A band.

Predictor variable	Definition	Ecological significance	Contribution to model (%)
Redness Index 200 m mean	Mean normalized difference of red and green band within 200 m window (Liu *et al.* 2018).	Ambiguous meaning as high values correlate with leaf senescence and dead vegetation but also bare soil (Liu *et al.* 2018). Coinciding high values of redness and CVI indicate sparse vegetation. Prey are more easily detected in sparse vegetation.	27.1
S08 TM Difference Variance 200 m sd	SD of texture metric for local heterogeneity within a 200 m grey level co-occurrence matrix (GLCM) of Sentinel band 8 (near infra-red – NIR). Defines the local heterogeneity by giving more weight to differing intensity level pairs (Haralick *et al.* 1973, Zwanenburg *et al.* 2020). High values (sd) ≙ high differences in local heterogeneity and vice versa.	The combination of NIR and green band carries information on ground vegetation. Variance in these bands codes variance in ground cover. Dotterels select for high heterogeneity (patchiness) in ground cover patterns.	27.1
Chlorophyll Vegetation Index (CVI) 200 m mean	Mean of Chlorophyll content in the vegetation within a 200 m cell (Vincini *et al.* 2008) based on NIR, red and green bands, corrected for patches of bare ground.	Identifies greening vegetation with high chlorophyll content even when interspersed with rocks or plant debris. Variable most linked to vegetation phenology. Hatching dates might be timed to vegetation phenology.	24.0
S04 200 m mean	Mean reflection of red band (Sentinel band 4) in a 200 m window.	Similar to redness index but less specific.	8.5
Topographic Wetness Index	Combines local upslope contributing area and slope to indicate the potential of runoff generation within catchment area. (Sørensen *et al.* 2006, Besnard *et al.* 2013).	High values indicate high potential for runoff generation and vice versa, highly correlated with soil moisture. Dotterels prefer flat, gently sloping ridges (Galbraith *et al.* 1993) with low runoff.	5.4
S03 TM Difference Variance 200 m mean	Texture metric for local heterogeneity within a 200 m grey level co-occurrence matrix (GLCM) of Sentinel band 3 (green band). Defines the local heterogeneity by giving more weight to differing intensity level pairs (Haralick *et al.* 1973, Zwanenburg *et al.* 2020). High values ≙ high local heterogeneity and vice versa.	The combination of NIR and green band carries information on ground vegetation. Variance in these bands codes variance in ground cover. Dotterels select for high heterogeneity (patchiness) in ground cover patterns.	4.1
Morphometric Protection Index 2,000 m	Algorithm that evaluates the protection or openness of a cell (Yokoyama & Pike 2002) in eight directions within a given radius (here 2,000 m) as a mean value. Low value ≙ low protection and high openness high value ≙ high protection and low openness (Watkins 2015).	Dotterels prefer exposed, elevated spots which are close to their preferred exposed foraging habitat, corresponding to low values of morphometric protection index.	3.8

to the highest quantile of CVI values attained in the study area (see Fig. 3). This implies a high chlorophyll concentration that represents the alpine meadows with their greening vegetation at the beginning of July, the acquisition date of the satellite images.

The *Redness Index* is the normalized difference between visible red and green band and is therefore a rather unspecific remote sensing product. It has been shown to be highly correlated with leaf senescence (Liu *et al.* 2018) and dead vegetation, but has also been successfully applied to monitor and predict bare soil and ground patterns (Mathieu *et al.* 1998). In the study area, the –0.18 isopleth of the redness index aligns well with the tree line. Maximum redness values close to or above zero occur on dry ridges with alpine meadows or unvegetated scree fields. Dotterels select for high redness values, yet due to its ambiguity, the redness index needs to be interpreted in combination with the CVI to understand dotterel preferences regarding ground vegetation type and phenology. Dotterels prefer areas where both indices are high, i.e. where vegetation is greening when their chicks hatch in the beginning of July, but at the same time is rather sparse and interspersed with rocks and plant debris from the previous summer. Dotterels may select habitats with sparse vegetation because prey are more easily detected. In our study areas males do most of the breeding and chick rearing (pers. obs.) and therefore can only make short foraging bouts and have to be extra vigilant, making it preferable to select breeding areas where prey are easily detected (Byrkjedal 1989, Holt *et al.* 2002).

The *Morphometric Protection Index* had the highest probability of occurrence with low values, which represent low protection and high openness of the surrounding area. This reflects a well-known component of the habitat of Dotterels, which prefer to nest on exposed, flat and gently sloping ridges (Galbraith *et al.* 1993, Holt 2002). Nesting in proximity to preferred foraging habitat that consists of exposed plant communities may play an important role for Dotterel nest site selection (Galbraith *et al.* 1993). The same applies to the *Topographic Wetness Index,* which contributes most with low values (Fig. 3). This implies a higher probability of presence on bare, dry ground that has been shown to be an important factor for the habitat of Dotterels (Galbraith *et al.* 1993).

The importance of the texture metric (*Sentinel band 3 Difference Variance 200 m mean*) indicates that local heterogeneity reflected in the green band does a good job at predicting suitable Dotterel habitat. The higher the reflectance heterogeneity, the higher the probability of presence for the Dotterel. The same is true for *Sentinel band 8 Difference Variance 200 m sd*: with an increasing standard deviation of local heterogeneity in the NIR band, the probability of presence increases. This implies an importance of heterogeneity within the cells: adjacent pixels within a 200 m cell have differing patterns, which creates a patchy mosaic within the cells. The habitat is characterized by a mosaic of bare ground, dead and green vegetation patterns that underlie differing environmental circumstances such as (permafrost) soil, snow melt, wind and rain exposition, rock cover etc. (Fig. 2). These locally heterogeneous patterns of differing vegetation cover and phenology, moss and lichen cover, bare ground, scattered rocks and debris are well-described as distinctive features of Dotterel habitat (e.g. Nethersole-Thompson 1972, Baxter 2016, Wiersma & Kirwan 2020). Breeding sites with higher small-scale heterogeneity may be selected because of proximity to preferred foraging habitats, the heterogeneous zone where bog and moss-heath intergrade, and a more diverse selection of prey items occur (Galbraith *et al.* 1993, Holt 2002). Consequently, breeding in heterogeneous habitats may play an important role in chick rearing, as the chicks can be easily guided to preferred foraging habitats. Heterogeneous habitats on the edge of bogs may also offer shelter and camouflage for the chicks, so they can be more easily hidden from bad weather and potential predators (Galbraith *et al.* 1993, Holt 2002). Similarly, European Golden Plover *Pluvialis apricaria* chicks in Vindelfjällen have been shown to prefer habitats with higher cover (willow scrub) possibly to minimize the risk of predation (Machin *et al.* 2019).

The availability of suitable breeding habitat for specialist species like the Dotterel on alpine plateaus within the Arctic tundra may decrease significantly in the future (Ewing *et al.* 2020). Small changes in environmental variables can have significant impacts on highly specialist species, whereas generalist species may adapt more easily and expand their range to new areas (Callaghan *et al.* 2011). The habitat composition within the Dotterel's present breeding range is predicted to change rapidly within the next decades, as is pointed out in studies on other Arctic-breeding species (Huntley 2007, Virkkala *et al.* 2014, Hayhow *et al.* 2015, Lindström *et al.* 2015). Altitudinal vegetation composition in mountain ranges has been shown to change as a consequence of several factors, for example climate change, grazing pressure and nitrogen deposition (Galbraith *et al.* 1993, Baxter 2016, Steinbauer *et al.* 2018). Consequentially, the openness of the Dotterel breeding habitat may decrease as taller shrubs and trees start growing higher on the tundra. Similarly, the habitat heterogeneity may decrease, with larger patches being covered by single species (e.g. dwarf birch or willows in our study area; pers. obs.).

Applying the model on a larger scale: implications for conservation

We used our model to estimate the population size in the entire Vindelfjällen Nature Reserve and predicted available suitable nesting habitat in approximately 1% of Vindelfjällen. When extrapolating our model results, this leads to a prediction of approximately 180 Dotterel nests/territories in the Nature Reserve. Given the high model performance and positive evaluation, this may be an accurate estimate of the size of the total breeding population of Dotterels in Vindelfjällen. The estimated population size for the Nature Reserve is equivalent to 4–9 % of the Swedish population estimate of 3,600 pairs (2,025–4,675; Ottosson *et al.* 2012). Ottosson *et al.* (2012) predicted the population of Lycksele

Lappmark county, where Vindelfjällen is situated, at 270 pairs. As the Vindelfjällen Nature Reserve comprises around 70% of the potentially suitable Arctic tundra above the treeline within Lycksele Lappmark, our extrapolation is well in line with that estimate. This is only a 'back-of-the-envelope' calculation, but the congruence with Ottosson *et al.*'s (2012) numbers shows that extrapolating ground surveys with detailed models on species habitat associations offers great potential for estimating population sizes in vast, inaccessible areas. For more detailed population predictions, a sensitivity analysis should investigate whether the threshold selection measure influences the predicted population size, to identify a robust estimation that is independent of the method used to delineate the species niche.

With detailed population surveys within the predicted Dotterel habitat, our model has great potential to serve as a tool for population estimations within bird monitoring schemes. Population densities however, should be validated by field surveys in different parts of the study species' distribution. With freely available satellite images and elevation models, our modeling approach may be applied to an arbitrarily large spatial context after further verification in other areas. This may have particular advantages over current population estimation methods that either use simple extrapolations without detailed species habitat associations, or have small sample sizes, possibly leading to high inaccuracies. To correctly estimate loss of suitable breeding habitat and population declines over larger scales, we advocate combining our model with climate-sensitive process-based vegetation models (e.g. Zhang *et al.* 2013). Using a time series of satellite images, our model can help to assess the quality of population estimates in a very time- and cost-efficient way. This is of particular interest considering the rapid climate change-driven changes in montane ecosystems, particularly in the Arctic (Chamberlain *et al.* 2013, Scridel *et al.* 2018). Since the Dotterel is a highly specialized species with a narrow ecological niche, predictions of suitable breeding habitat using remote sensing data are relatively straightforward. Our modelling approach should be verified with other, more generalist species in different study areas to assess the breadth of potential ecotypes. Niche delineation might be harder and prediction power thus lower for more generalist species. We highly recommend repeating the model evaluation process with independent data whenever applying the model to other areas or species.

Applying the distribution models presented here to more species in different areas will increase our knowledge of the present distribution of species. With future research, distribution patterns may be combined with climate change models, allowing detailed predictions of shifts in availability of suitable breeding habitat and consequent changes in population size for Arctic-breeding shorebirds of conservation concern.

ACKNOWLEDGEMENTS

We thank the International Wader Study Group (IWSG) for financial support for our field work in 2019 through the small grant program. The research was partly funded by the Hessen State Ministry for Higher Education, Research and the Arts, Germany, as part of the LOEWE priority project Nature 4.0 – Sensing Biodiversity. We thank Samantha Franks, Steven Ewing and John Atle Kålås for their constructive revision and helpful comments on earlier versions of this manuscript. We thank Åke Lindström from Lund University for inviting us to carry out fieldwork on Dotterels in Vindelfjällen Nature Reserve. We further thank Sophie Ehnbom for providing further Dotterel breeding locations for the model validation. We thank Rob van Bemmelen, Linus Hedh, Noel Hohenthal, Marie Kordilla, Erik Owusu-Ansah, Alexandra Munters, Morrison Pot, Jan Sohler and Birgith Unterthurner for their passionate work during the field seasons and the great time spent together in the Arctic wilderness.

ONLINE SUPPLEMENTARY INFORMATION

Table S1. Remote sensing data derived indices as input for the variable selection procedure.

REFERENCES

Baugh, W.M. & D.P. Groeneveld. 2006. Broadband vegetation index performance evaluated for a low-cover environment. *International Journal of Remote Sensing* 27: 4715–4730.

Baxter, A. 2016. *Understanding the factors associated with declines of an alpine specialist bird species in Scotland*. PhD thesis, University of Aberdeen, UK.

Besnard, A.G., I. La Jeunesse, O. Pays & J. Secondi. 2013. Topographic wetness index predicts the occurrence of bird species in floodplains. *Diversity & Distributions* 19: 955–963.

BirdLife International. 2019. *Important Bird Areas factsheet: Vindel Mountains (including Lake Tärna).* Accessed 9 May 2021 at: *http://datazone.birdlife.org/site/factsheet/vindel-mountains-(including-lake-tärna)-iba-sweden/refs*

BirdLife International. 2021. *BirdLife species factsheet: Eurasian Dotterel (Eudromias morinellus)* Accessed 9 May 2021 at: *http://datazone.birdlife.org/species/factsheet/22693906*

Byrkjedal, I. 1989. Time constraints and vigilance: Breeding season diet of the Dotterel (*Charadrius morinellus*). *Journal für Ornithologie* 130: 293–302.

Callaghan, T.V., M. Johansson, R.D. Brown, P.Ya. Groisman, N. Labba, … & E.F. Wood. 2011. Multiple effects of changes in Arctic snow cover. *AMBIO* 40: 32–45.

Chamberlain, D.E., M. Negro, E. Caprio & A. Rolando. 2013. Assessing the sensitivity of alpine birds to potential future changes in habitat and climate to inform management strategies. *Biological Conservation* 167: 127–135.

Chen, I-C., J.K. Hill, R. Ohlemüller, D.B. Roy & C.D. Thomas. 2011. Rapid range shifts of species associated with high levels of climate warming. *Science* 333: 1024–1026.

Conrad, O., B. Bechtel, M. Bock, H. Dietrich, E. Fischer, L. Gerlitz, J. Wehberg, V. Wichmann & J. Böhner. 2015. System for automated geoscientific analyses (SAGA) v. 2.1.4. *Geoscientific Model Development Discussions* 8: 2271–2312.

Di Cola, V., O. Broennimann, B. Petitpierre, C. Randin, R. Engler, A. Dubuis, M. D'Amen, L. Pellissier, J. Pottier, D. Pio, N. Salamin, F. Breiner, R. Mateo, W. Hordijk & A.

Guisan. 2017. ecospat: An R package to support spatial analyses and modeling of species niches and distributions. *Ecography* 40: 774–787.

Eaton, M., N. Aebischer, A. Brown, R. Hearn, L. Lock, A. Musgrove, D. Noble, D. Stroud & R. Gregory. 2015. Birds of conservation concern 4: the population status of birds in the UK, Channel Islands and Isle of Man. *British Birds* 108: 708–746.

Engler, J., D. Rödder, O. Elle, A. Hochkirch & J. Secondi. 2013. Species distribution models contribute to determine the effect of climate and interspecific interactions in moving hybrid zones. *Journal of Evolutionary Biology* 26: 2487–2496.

Escalante, T., G. Rodríguez-Tapia, M. Linaje, P. Illoldi & R. González. 2013. Identification of areas of endemism from species distribution models: Threshold selection and Nearctic mammals. *Revista Especializada en Ciencias Químico-Biológicas* 16: 5–17.

Ewing, S., A. Baxter, J. Wilson, D. Hayhow, J. Gordon, D. Thompson, D. Whitfield & R. van der Wal. 2020. Clinging on to alpine life: Investigating factors driving the uphill range contraction and population decline of a mountain breeding bird. *Global Change Biology* 26: 3771–3787.

Fourcade, Y., J.O. Engler, D. Rödder & J. Secondi. 2014. Mapping species distributions with MAXENT using a geographically biased sample of presence data: a performance assessment of methods for correcting sampling bias. *PLoS ONE* 9: e97122.

Galbraith, H., S. Murray, S. Rae, D.P. Whitfield & D.B.A. Thompson. 1993. Numbers and distribution of Dotterel *Charadrius morinellus* breeding in Great Britain. *Bird Study* 40: 161–169.

Gejl, L. 2017. *Waders of Europe*. Bloomsbury Publishing PLC, London, UK.

Gottwald, J., T. Appelhans, F. Adorf, J. Hillen & T. Nauss. 2017. High-resolution MaxEnt modelling of habitat suitability for maternity colonies of the Barbastelle Bat *Barbastella barbastellus* (Schreber, 1774) in Rhineland-Palatinate, Germany. *Acta Chiropterologica* 19: 389–398.

Hampe, A. & R. Petit. 2005. Conserving biodiversity under climate change: The rear edge matters. *Ecology Letters* 8: 461–467.

Haralick, R., K. Shanmugam & I. Dinstein. 1973. Textural features for image classification. *IEEE Transactions on Systems, Man, and Cybernetics* SMC-3: 610–621.

Hayhow, D.B., S.R. Ewing, A. Baxter, A. Douse, A. Stanbury, D.P. Whitfield & M.A. Eaton. 2015. Changes in the abundance and distribution of a montane specialist bird, the Dotterel *Charadrius morinellus*, in the UK over 25 years. *Bird Study* 62: 443–456.

Hijmans, R.J., S. Phillips, J. Leathwick & J. Elith. 2021. *Dismo: Species distribution modeling.* R package v.1.3-5.

Hirzel, A., G. Lay, V. Helfer, C. Randin & A. Guisan. 2006. Evaluating the ability of habitat suitability models to predict species presences. *Ecological Modelling* 199: 142–152.

Hof, A., G. Rodriguez-Castaneda, A. Allen, R. Jansson & C. Nilsson. 2016. Vulnerability of Subarctic and Arctic breeding birds. *Ecological Applications* 27: 219–234.

Holt, S. 2002. *Uniparental incubation in a cool climate: behavioural adaptations in the Eurasian Dotterel.* PhD thesis, University of Stirling, UK.

Holt, S., D.P. Whitfield & J. Gordon. 2002. Potential reproductive rates in the Eurasian Dotterel *Charadrius morinellus*. *Bird Study* 49: 87–88.

Høye, T. & M. Forchhammer. 2008. Phenology of High-Arctic arthropods: Effects of climate on spatial, seasonal, and inter-annual variation. *Advances in Ecological Research* 40: 299–324.

Huntley, B., R.E. Green, Y.C. Collingham & S.G. Willis. 2007. *A climatic atlas of European breeding birds.* Lynx Editions, Barcelona, Spain.

Kerr, J. & M. Ostrovsky. 2003. From space to species: Ecological applications for remote sensing. *Trends in Ecology & Evolution* 18: 299–305.

Kupidura, P. 2019. The comparison of different methods of texture analysis for their efficacy for land use classification in satellite imagery. *Remote Sensing* 11: 1233.

Lathrop, R., L. Niles, P. Smith, M. Peck, A. Dey, R. Sacatelli & J. Bognar. 2018. Mapping and modeling the breeding habitat of the Western Atlantic Red Knot (*Calidris canutus rufa*) at local and regional scales. *Condor* 120: 650–665.

Lehikoinen, A., L. Brotons, J. Calladine, T. Campedelli, V. Escandell, … & S. Trautmann. 2018. Declining population trends of European mountain birds. *Global Change Biology* 25: 577–588.

Leitão, P. & M. Santos. 2019. Improving models of species ecological niches: A remote sensing overview. *Frontiers in Ecology & Evolution* 7: 9.

Lindström, Å., M. Green, G. Paulson, H. Smith & V. Devictor. 2013. Rapid changes in bird community composition at multiple spatial scales in response to recent climate change. *Ecography* 36: 313–322.

Lindström, Å., M. Green, M. Husby, J.A. Kålås & A. Lehikoinen. 2015. Large-scale monitoring of waders on their Boreal and Arctic breeding grounds in Northern Europe. *Ardea* 103: 3–15.

Lindström, Å., M. Green, M. Husby, J. Kålås, A. Lehikoinen & M. Stjernman. 2019. Population trends of waders on their boreal and arctic breeding grounds in northern Europe. *Wader Study* 126: 200–216.

Liu, Z., S. An, X. Lu, H. Hu & J. Tang. 2018. Using canopy greenness index to identify leaf ecophysiological traits during the foliar senescence in an oak forest. *Ecosphere* 9: e02337.

Lu, D., G. Li, E. Moran, L. Dutra & M. Batistella. 2014. The roles of textural images in improving land-cover classification in the Brazilian Amazon. *International Journal of Remote Sensing* 35: 8188–8207.

Machin, P., J. Fernández-Elipe, J. Hungar, A. Angerbjörn, R. Klaassen & J. Aguirre. 2019. The role of ecological and environmental conditions on the nesting success of waders in sub-Arctic Sweden. *Polar Biology* 42: 1571–1579.

Marchant, J., P. Hayman & A. Prater. 1986. *Shorebirds: An identification guide to the waders of the world.* Houghton Mifflin Harcourt, Boston, MA, USA.

Mathieu, R., M. Pouget, B. Cervelle & R. Escadafal. 1998. Relationships between satellite-based radiometric indices simulated using laboratory reflectance data and typic soil color of an arid environment. *Remote Sensing of Environment* 66: 17–28.

Merow, C., M. Smith & J. Silander. 2013. A practical guide to MaxEnt for modeling species' distributions: What it does,

and why inputs and settings matter. *Ecography* 36: 1058–1069.

Meyer, H., C. Reudenbach, T. Hengl, M. Katurji & T. Nauss. 2018. Improving performance of spatio-temporal machine learning models using forward feature selection and target-oriented validation. *Environmental Modelling & Software* 101: 1–9.

Montenegro, C., L. Solitario, S. Manglar & D. Guinto. 2017. Niche modelling of endangered Philippine birds using GARP and MAXENT. In: *7th International Conference on Cloud Computing, Data Science & Engineering-Confluence*. IEEE, Noida, India.

Morales, N.S., I.C. Fernández & V. Baca-González. 2017. MaxEnt's parameter configuration and small samples: are we paying attention to recommendations? A systematic review. *PeerJ* 5: e3093.

Nethersole-Thompson, D. 1972. *The Dotterel, 1st Edn*. Harper-Collins, London, UK.

Ottosson, U., R. Ottvall, M. Green, R. Gustafsson, F. Haas, H. Niklas, Å. Lindström, L. Nilsson, S. Mikael, S. Svensson & M. Tjernberg. 2012. *Fåglarna i Sverige- antal och förekomst.* Sveriges Ornitologiska Förening, Sweden. [In Swedish]

Phillips, S. & M. Dudík. 2008. Modeling of species distributions with MAXENT: new extensions and a comprehensive evaluation. *Ecography* 31: 161–175.

Phillips, S., R. Anderson & R. Schapire. 2006. Maximum entropy modeling of species geographic distribution. *Ecological Modelling* 190: 231–259.

Phillips, S., R. Anderson, M. DudÍk, R. Schapire & M. Blair. 2017. Opening the black box: An open-source release of Maxent. *Ecography* 40: 887–893.

Puletti, N., F. Chianucci & C. Castaldi. 2017. Use of Sentinel-2 for forest classification in Mediterranean environments. *Annals of Silvicultural Research* 42: 32–38.

QGIS Development Team. 2021. *QGIS Geographic Information System*. QGIS Association. Available at: *http://www.qgis.org*

R Core Team. 2020. *R: A Language and Environment for Statistical Computing*. R Foundation for Statistical Computing, Vienna, Austria.

Saalfeld, S., R. Lanctot, S. Brown, D. Saalfeld, J. Johnson, B. Andres & J. Bart. 2013. Predicting breeding shorebird distributions on the Arctic Coastal Plain of Alaska. *Ecosphere* 12: e03761.

Scridel, D., G. Bogliani, P. Pedrini, A. Iemma, A. von Hardenberg & M. Brambilla. 2017. Thermal niche predicts recent changes in range size for bird species. *Climate Research* 73: 207–216.

Scridel, D., M. Brambilla, K. Martin, A. Lehikoinen, A. Iemma, A. Matteo, S. Jähnig, E. Caprio, G. Bogliani, P. Pedrini, A. Rolando, R. Arlettaz & D. Chamberlain. 2018. A review and meta-analysis of the effects of climate change on Holarctic mountain and upland bird populations. *Ibis* 160: 489–515.

Sørensen, R., U. Zinko & J. Seibert. 2006. On the calculation of the topographic wetness index: Evaluation of different methods based on field observations. *Hydrology & Earth System Sciences* 10: 101–112.

Staafjord, T. 2012. *Vindelfjällens naturreservat, Grundutredning om natur, kultur, nyttjande och förvaltning.* Nature reserve report Länsstyrelsen Västerbotten, Sweden. [In Swedish]

Steinbauer, M., J.A. Grytnes, G. Jurasinski, A. Kulonen, J. Lenoir, … & S. Wipf. 2018. Accelerated increase in plant species richness on mountain summits is linked to warming. *Nature* 556: 231–234.

Svensson, S. & T. Andersson. 2013. Population trends of birds in alpine habitats at Ammarnäs in southern Swedish Lapland 1972–2011. *Ornis Svecica* 23: 81–107.

Tulp, I. & H. Schekkerman. 2008. Has prey availability for Arctic birds advanced with climate change? Hindcasting the abundance of tundra arthropods using weather and seasonal variations. *Arctic* 61: 48–60.

Urban, M. 2015. Climate change. Accelerating extinction risk from climate change. *Science* 348: 571–573.

Vilà-Cabrera, A., A. Premoli & A. Jump. 2019. Refining predictions of population decline at species' rear edges. *Global Change Biology* 25: 1549–1560.

Vincini, M., E. Frazzi & P. D'Alessio. 2008. A broad-band leaf chlorophyll vegetation index at the canopy scale. *Precision Agriculture* 9: 303–319.

Virkkala, R., R. Heikkinen, A. Lehikoinen & J. Valkama. 2014. Matching trends between recent distributional changes of northern-boreal birds and species-climate model predictions. *Biological Conservation* 172: 124–127.

Warren, D. & S. Seifert. 2011. Ecological niche modeling in Maxent: the importance of model complexity and the performance of model selection criteria. *Ecological Applications* 21: 335–342.

Watkins, R. 2015. *Terrain metrics and landscape characterization from bathymetric data: SAGA GIS methods and command sequences*. Report to Pacific Islands Fisheries Science Center, Honolulu, HI, USA.

Wauchope, H., J. Shaw, Ø. Varpe, E. Lappo, D. Boertmann, R. Lanctot & R. Fuller. 2016. Rapid climate-driven loss of breeding habitat for Arctic migratory birds. *Global Change Biology* 23: 1085–1094.

Whitfield, D.P. 2002. Status of breeding Dotterel *Charadrius morinellus* in Britain in 1999. *Bird Study* 49: 237–249.

Wiersma, P. & G.M. Kirwan. 2020. Eurasian Dotterel (*Charadrius morinellus*), v.1.0. In: *Birds of the World* (J. del Hoyo, A. Elliott, J. Sargatal, D.A. Christie & E. de Juana, Eds.). Cornell Lab of Ornithology, Ithaca, NY, USA. Accessed 9 May 2021 at: *https://doi.org/10.2173/bow.eurdot.01*

Yokoyama, R. & R. Pike. 2002. Visualizing topography by openness: A new application of image processing to digital elevation models. *Photogrammetric Engineering & Remote Sensing* 68: 257–266.

Zeng, Y., B.W. Low & D. Yeo. 2016. Novel methods to select environmental variables in MaxEnt: A case study using invasive crayfish. *Ecological Modelling* 341: 5–13.

Zhang, W., P. Miller, B. Smith, R. Wania, T. Koenigk & R. Döscher. 2013. Tundra shrubification and tree-line advance amplify arctic climate warming: Results from an individual-based dynamic vegetation model. *Environmental Research Letters* 8: 1–10.

Zwanenburg, A., M. Vallières, M. Abdalah, H. Aerts, V. Andrearczyk, … & S. Löck. 2020**.** The image biomarker standardization initiative: Standardized quantitative radiomics for high-throughput image-based phenotyping. *Radiology* 295: 328–338**.**

research paper *Wader Study* 128(3): supplement. doi:10.18194/ws.00250

Supplementary material for

Exploring the Dotterel Mountains: Improving the understanding of breeding habitat characteristics of an Arctic-breeding specialist bird

Christian Hoefs, Tim van der Meer, Peter Antkowiak, Jonas Hagge, Martin Green & Jannis Gottwald

Corresponding author: christianhoefs@gmail.com

This PDF contains:

Table S1. Remote sensing data derived indices as input for the variable selection procedure.

Table S1. Remote sensing data derived indices as input for the variable selection procedure (see *Methods*). The dataset comprised 42 spectral indices, 154 texture metrics and 15 topographic indices.

	Abbreviation	Name
Spectral (Vegetation) Indices	ARVIidx	Atmospherically Resistant Vegetation Index
	ARVIidx_200m_mean	Atmospherically Resistant Vegetation Index 200m standard deviation
	ARVIidx_200m_sd	Atmospherically Resistant Vegetation Index 200m mean
	B02	Sentinel Band 2
	B02_200m_mean	Sentinel Band 200m mean
	B03	Sentinel Band 3
	B03_200m_mean	Sentinel Band 3 200m mean
	B03_200m_sd	Sentinel Band 3 200m standard deviation
	B04	Sentinel Band 4
	B04_200m_mean	Sentinel Band 4 200m mean
	B04_200m_sd	Sentinel Band 4 200m standard deviation
	B08	Sentinel Band 8
	B08_200m_mean	Sentinel Band 8 200m mean
	B08_200m_sd	Sentinel Band 8 200m standard deviation
	BWDRVIidx	Blue-wide dynamic range vegetation index
	BWDRVIidx_200m_mean	Blue-wide dynamic range vegetation index mean
	BWDRVIidx_200m_sd	Blue-wide dynamic range vegetation index 200m standard deviation
	CVIidx	Chlorophyll Vegetation Index
	CVIidx_200m_mean	Chlorophyll Vegetation Index 200m mean
	CVIidx_200m_sd	Chlorophyll Vegetation Index 200m standard deviation
	EVIidx	Enhanced Vegetation Index
	EVIidx_200m_mean	Enhanced Vegetation Index 200m mean
	EVIidx_200m_sd	Enhanced Vegetation Index 200m standard deviation
	EVIidx2_200m_mean	Enhanced Vegetation Index 2 200m mean
	EVIidx2_200m_sd	Enhanced Vegetation Index 2 200m standard deviation
	green_leaf_idx	Grean Leaf Index
	green_leaf_idx_200m_mean	Grean Leaf Index 200m mean
	green_leaf_idx_200m_sd	Grean Leaf Index 200m standard deviation
	intensity_idx	Intensity Index
	intensity_idx_200m_mean	Intensity Index 200m mean
	intensity_idx_200m_sd	Intensity Index 200m standard deviation
	NDVIidx	Normalized Difference Vegetation Index
	NDVIidx_200m_mean	Normalized Difference Vegetation Index 200m mean
	NDVIidx_200m_sd	Normalized Difference Vegetation Index 200m standard deviation
	redness_idx	Redness Index
	redness_idx_200m_mean	Redness Index
	redness_idx_200m_sd	Redness Index
	rgb_shape_idx	Colour and Shape Index
	rgb_shape_idx_200m_sd	Colour and Shape Index 200m standard deviation
	VVIidx	Visible Vegetation Index
	VVIidx_200m_mean	Visible Vegetation Index 200m mean
	VVIidx_200m_sd	Visible Vegetation Index 200m standard deviation

Table S1, continued

	Abbreviation	Name
Topographic Indices	slope	Slope
	slope_100_mean	Slope 100m mean
	topographic_position_ind_ex1000	Topographic Position Index 1000m
	topographic_position_ind_ex2000	Topographic Position Index 2500m
	topographic_position_ind_ex250	Topographic Position Index 250m
	topographic_wetness_idx_0	Topographic Wetness Index
	topographic_wetness_idx_1	Topographic Wetness Index 200 m
	aspect	Aspect
	aspect_100_mean	Aspect 100m mean
	protection1000_resamp	Morphometric Protection Index 1000m
	protection2000_resamp	Morphometric Protection Index 2000m
	protection250_resamp	Morphometric Protection Index 250m
	dem	Digital Elevation Model
	curvature	Curvature
	curvature_100_mean	Curvature 100m mean
Structural Indices (Texture Metrics)	B03_hara_ASM 0.0355	Sentinel Band 3 Haralick Angular Second Moment
	B03_hara_ASM_200m_mean	Sentinel Band 3 Haralick Angular Second Moment 200 m mean
	B03_hara_ASM_200m_sd	Sentinel Band 3 Haralick Angular Second Moment 200 m standard deviation
	B03_hara_Contr 0.0043	Sentinel Band 3 Haralick Contrast
	B03_hara_Contr_200m_mean	Sentinel Band 3 Haralick Contrast 200 m mean
	B03_hara_Contr_200m_sd	Sentinel Band 3 Haralick Contrast 200 m standard deviation
	B03_hara_Corr 0.0535	Sentinel Band 3 Haralick Correlation
	B03_hara_Corr_200m_mean	Sentinel Band 3 Haralick Correlation 200 m mean
	B03_hara_Corr_200m_sd	Sentinel Band 3 Haralick Correlation 200 m standard deviation
	B03_hara_DE 0.1521	Sentinel Band 3 Haralick Difference Entropy
	B03_hara_DE_200m_mean	Sentinel Band 3 Haralick Difference Entropy 200 m mean
	B03_hara_DE_200m_sd	Sentinel Band 3 Haralick Difference Entropy 200 m standard deviation
	B03_hara_DV 0.1465	Sentinel Band 3 Haralick Difference Variance
	B03_hara_DV_200m_mean	Sentinel Band 3 Haralick Difference Variance 200 m mean
	B03_hara_DV_200m_sd	Sentinel Band 3 Haralick Difference Variance 200 m standard deviation
	B03_hara_Entr 0.0077	Sentinel Band 3 Haralick Entropy
	B03_hara_Entr_200m_mean	Sentinel Band 3 Haralick Entropy 200 m mean
	B03_hara_Entr_200m_sd	Sentinel Band 3 Haralick Entropy 200 m standard deviation
	B03_hara_IDM 0.0368	Sentinel Band 3 Haralick Inverse Difference Moment
	B03_hara_IDM_200m_mean	Sentinel Band 3 Haralick Inverse Difference Moment 200 m mean
	B03_hara_IDM_200m_sd	Sentinel Band 3 Haralick Inverse Difference Moment 200 m standard deviation
	B03_hara_MOC.1 0.0227	Sentinel Band 3 Haralick Information Measures of Correlation 1
	B03_hara_MOC.1_200m_mean	Sentinel Band 3 Haralick Information Measures of Correlation 1 200 m mean
	B03_hara_MOC.1_200m_sd	Sentinel Band 3 Haralick Information Measures of Correlation 1 200 m standard deviation
	B03_hara_MOC.2 0.0465	Sentinel Band 3 Haralick Information Measures of Correlation 2
	B03_hara_MOC.2_200m_mean	Sentinel Band 3 Haralick Information Measures of Correlation 2 200 m mean
	B03_hara_MOC.2_200m_sd	Sentinel Band 3 Haralick Information Measures of Correlation 2 200 m standard deviation

Table S1, continued

	Abbreviation	Name
Structural Indices (Texture Metrics)	B03_hara_SA 0.0479	Sentinel Band 3 Haralick Sum Average
	B03_hara_SA_200m_mean	Sentinel Band 3 Haralick Sum Average 200 m mean
	B03_hara_SA_200m_sd	Sentinel Band 3 Haralick Sum Average 200 m standard deviation
	B03_hara_SE 0.0050	Sentinel Band 3 Haralick Sum Entropy
	B03_hara_SE_200m_mean	Sentinel Band 3 Haralick Sum Entropy 200 m mean
	B03_hara_SE_200m_sd	Sentinel Band 3 Haralick Sum Entropy 200 m standard deviation
	B03_hara_SV 0.0002	Sentinel Band 3 Haralick Sum Variance
	B03_hara_SV_200m_mean	Sentinel Band 3 Haralick Sum Variance 200 m mean
	B03_hara_SV_200m_sd	Sentinel Band 3 Haralick Sum Variance 200 m standard deviation
	B03_hara_Var 0.0001	Sentinel Band 3 Haralick Variance
	B03_hara_Var_200m_mean	Sentinel Band 3 Haralick Variance 200 m mean
	B03_hara_Var_200m_sd	Sentinel Band 3 Haralick Variance 200 m standard deviation
	B08_hara_ASM 0.0089	Sentinel Band 8 Haralick Angular Second Moment
	B08_hara_ASM_200m_mean	Sentinel Band 8 Haralick Angular Second Moment 200 m mean
	B08_hara_ASM_200m_sd	Sentinel Band 8 Haralick Angular Second Moment 200 m standard deviation
	B08_hara_Contr 0.0000	Sentinel Band 8 Haralick Contrast
	B08_hara_Contr_200m_mean	Sentinel Band 8 Haralick Contrast 200 m mean
	B08_hara_Contr_200m_sd	Sentinel Band 8 Haralick Contrast 200 m standard deviation
	B08_hara_Corr 0.2416	Sentinel Band 8 Haralick Correlation
	B08_hara_Corr_200m_mean	Sentinel Band 8 Haralick Correlation 200 m mean
	B08_hara_Corr_200m_sd	Sentinel Band 8 Haralick Correlation 200 m standard deviation
	B08_hara_DE 0.0335	Sentinel Band 8 Haralick Difference Entropy
	B08_hara_DE_200m_mean	Sentinel Band 8 Haralick Difference Entropy 200 m mean
	B08_hara_DE_200m_sd	Sentinel Band 8 Haralick Difference Entropy 200 m standard deviation
	B08_hara_DV 0.0573	Sentinel Band 8 Haralick Difference Variance
	B08_hara_DV_200m_mean	Sentinel Band 8 Haralick Difference Variance 200 m mean
	B08_hara_DV_200m_sd	Sentinel Band 8 Haralick Difference Variance 200 m standard deviation
	B08_hara_Entr 0.0000	Sentinel Band 8 Haralick Entropy
	B08_hara_Entr_200m_mean	Sentinel Band 8 Haralick Entropy 200 m mean
	B08_hara_Entr_200m_sd	Sentinel Band 8 Haralick Entropy 200 m standard deviation
	B08_hara_IDM 0.0103	Sentinel Band 8 Haralick Inverse Difference Moment
	B08_hara_IDM_200m_mean	Sentinel Band 8 Haralick Inverse Difference Moment 200 m mean
	B08_hara_IDM_200m_sd	Sentinel Band 8 Haralick Inverse Difference Moment 200 m standard deviation
	B08_hara_MOC.1 0.0306	Sentinel Band 8 Haralick Information Measures of Correlation 1
	B08_hara_MOC.1_200m_mean	Sentinel Band 8 Haralick Information Measures of Correlation 1 200 m mean
	B08_hara_MOC.1_200m_sd	Sentinel Band 8 Haralick Information Measures of Correlation 1 200 m standard deviation
	B08_hara_MOC.2 0.0679	Sentinel Band 8 Haralick Information Measures of Correlation 2
	B08_hara_MOC.2_200m_mean	Sentinel Band 8 Haralick Information Measures of Correlation 2 200 m mean
	B08_hara_MOC.2_200m_sd	Sentinel Band 8 Haralick Information Measures of Correlation 2 200 m standard deviation
	B08_hara_SA 0.0496	Sentinel Band 8 Haralick Sum Average
	B08_hara_SA_200m_mean	Sentinel Band 8 Haralick Sum Average 200 m mean
	B08_hara_SA_200m_sd	Sentinel Band 8 Haralick Sum Average 200 m standard deviation

Table S1, continued

	Abbreviation	Name
Structural Indices (Texture Metrics)	B08_hara_SE 0.0199	Sentinel Band 8 Haralick Sum Entropy
	B08_hara_SE_200m_mean	Sentinel Band 8 Haralick Sum Entropy 200 m mean
	B08_hara_SE_200m_sd	Sentinel Band 8 Haralick Sum Entropy 200 m standard deviation
	B08_hara_SV 0.0731	Sentinel Band 8 Haralick Sum Variance
	B08_hara_SV_200m_mean	Sentinel Band 8 Haralick Sum Variance 200 m mean
	B08_hara_SV_200m_sd	Sentinel Band 8 Haralick Sum Variance 200 m standard deviation
	B08_hara_Var 0.0001	Sentinel Band 8 Haralick Variance
	B08_hara_Var_200m_mean	Sentinel Band 8 Haralick Variance 200 m mean
	B08_hara_Var_200m_sd	Sentinel Band 8 Haralick Variance 200 m standard deviation
	B04_hara_ASM 0.1273	Sentinel Band 4 Haralick Angular Second Moment
	B04_hara_ASM_200m_mean	Sentinel Band 4 Haralick Angular Second Moment 200 m mean
	B04_hara_ASM_200m_sd	Sentinel Band 4 Haralick Angular Second Moment 200 m standard deviation
	B04_hara_Contr 0	Sentinel Band 4 Haralick Contrast
	B04_hara_Contr_200m_mean	Sentinel Band 4 Haralick Contrast 200 m mean
	B04_hara_Contr_200m_sd	Sentinel Band 4 Haralick Contrast 200 m standard deviation
	B04_hara_Corr 0.1353	Sentinel Band 4 Haralick Correlation
	B04_hara_Corr_200m_mean	Sentinel Band 4 Haralick Correlation 200 m mean
	B04_hara_Corr_200m_sd	Sentinel Band 4 Haralick Correlation 200 m standard deviation
	B04_hara_DE 0.4402	Sentinel Band 4 Haralick Difference Entropy
	B04_hara_DE_200m_mean	Sentinel Band 4 Haralick Difference Entropy 200 m mean
	B04_hara_DE_200m_sd	Sentinel Band 4 Haralick Difference Entropy 200 m standard deviation
	B04_hara_DV 0.0647	Sentinel Band 4 Haralick Difference Variance
	B04_hara_DV_200m_mean	Sentinel Band 4 Haralick Difference Variance 200 m mean
	B04_hara_DV_200m_sd	Sentinel Band 4 Haralick Difference Variance 200 m standard deviation
	B04_hara_Entr 0.0018	Sentinel Band 4 Haralick Entropy
	B04_hara_Entr_200m_mean	Sentinel Band 4 Haralick Entropy 200 m mean
	B04_hara_Entr_200m_sd	Sentinel Band 4 Haralick Entropy 200 m standard deviation
	B04_hara_IDM 0.1258	Sentinel Band 4 Haralick Inverse Difference Moment
	B04_hara_IDM_200m_mean	Sentinel Band 4 Haralick Inverse Difference Moment 200 m mean
	B04_hara_IDM_200m_sd	Sentinel Band 4 Haralick Inverse Difference Moment 200 m standard deviation
	B04_hara_MOC.1 0.0587	Sentinel Band 4 Haralick Information Measures of Correlation 1
	B04_hara_MOC.1_200m_mean	Sentinel Band 4 Haralick Information Measures of Correlation 1 200 m mean
	B04_hara_MOC.1_200m_sd	Sentinel Band 4 Haralick Information Measures of Correlation 1 200 m standard deviation
	B04_hara_MOC.2 0.0421	Sentinel Band 4 Haralick Information Measures of Correlation 2
	B04_hara_MOC.2_200m_mean	Sentinel Band 4 Haralick Information Measures of Correlation 2 200 m mean
	B04_hara_MOC.2_200m_sd	Sentinel Band 4 Haralick Information Measures of Correlation 2 200 m standard deviation
	B04_hara_SA 0.0844	Sentinel Band 4 Haralick Sum Average
	B04_hara_SA_200m_mean	Sentinel Band 4 Haralick Sum Average 200 m mean
	B04_hara_SA_200m_sd	Sentinel Band 4 Haralick Sum Average 200 m standard deviation
	B04_hara_SE 0.0336	Sentinel Band 4 Haralick Sum Entropy
	B04_hara_SE_200m_mean	Sentinel Band 4 Haralick Sum Entropy 200 m mean
	B04_hara_SE_200m_sd	Sentinel Band 4 Haralick Sum Entropy 200 m standard deviation

Table S1, continued

	Abbreviation	Name
Structural Indices (Texture Metrics)	B04_hara_SV 0.0356	Sentinel Band 4 Haralick Sum Variance
	B04_hara_SV_200m_mean	Sentinel Band 4 Haralick Sum Variance 200 m mean
	B04_hara_SV_200m_sd	Sentinel Band 4 Haralick Sum Variance 200 m standard deviation
	B04_hara_Var 0.0000	Sentinel Band 4 Haralick Variance
	B04_hara_Var_200m_mean	Sentinel Band 4 Haralick Variance 200 m mean
	B04_hara_Var_200m_sd	Sentinel Band 4 Haralick Variance 200 m standard deviation
	B02_hara_ASM 0.0766	Sentinel Band 2 Haralick Angular Second Moment
	B02_hara_ASM_200m_mean	Sentinel Band 2 Haralick Angular Second Moment 200 m mean
	B02_hara_ASM_200m_sd	Sentinel Band 2 Haralick Angular Second Moment 200 m standard deviation
	B02_hara_Contr 0.1326	Sentinel Band 2 Haralick Contrast
	B02_hara_Contr_200m_mean	Sentinel Band 2 Haralick Contrast 200 m mean
	B02_hara_Contr_200m_sd	Sentinel Band 2 Haralick Contrast 200 m standard deviation
	B02_hara_Corr 0.2370	Sentinel Band 2 Haralick Correlation
	B02_hara_Corr_200m_mean	Sentinel Band 2 Haralick Correlation 200 m mean
	B02_hara_Corr_200m_sd	Sentinel Band 2 Haralick Correlation 200 m standard deviation
	B02_hara_DE 0.0577	Sentinel Band 2 Haralick Difference Entropy
	B02_hara_DE_200m_mean	Sentinel Band 2 Haralick Difference Entropy 200 m mean
	B02_hara_DE_200m_sd	Sentinel Band 2 Haralick Difference Entropy 200 m standard deviation
	B02_hara_DV 0.0484	Sentinel Band 2 Haralick Difference Variance
	B02_hara_DV_200m_mean	Sentinel Band 2 Haralick Difference Variance 200 m mean
	B02_hara_DV_200m_sd	Sentinel Band 2 Haralick Difference Variance 200 m standard deviation
	B02_hara_Entr 0.0032	Sentinel Band 2 Haralick Entropy
	B02_hara_Entr_200m_mean	Sentinel Band 2 Haralick Entropy 200 m mean
	B02_hara_Entr_200m_sd	Sentinel Band 2 Haralick Entropy 200 m standard deviation
	B02_hara_IDM 0.0030	Sentinel Band 2 Haralick Inverse Difference Moment
	B02_hara_IDM_200m_mean	Sentinel Band 2 Haralick Inverse Difference Moment 200 m mean
	B02_hara_IDM_200m_sd	Sentinel Band 2 Haralick Inverse Difference Moment 200 m standard deviation
	B02_hara_MOC.1 0.0323	Sentinel Band 2 Haralick Information Measures of Correlation 1
	B02_hara_MOC.1_200m_sd	Sentinel Band 2 Haralick Information Measures of Correlation 1 200 m standard deviation
	B02_hara_MOC.2 0.0909	Sentinel Band 2 Haralick Information Measures of Correlation 2
	B02_hara_MOC.2_200m_sd	Sentinel Band 2 Haralick Information Measures of Correlation 2 200 m standard deviation
	B02_hara_SA 0.9080	Sentinel Band 2 Haralick Sum Average
	B02_hara_SA_200m_mean	Sentinel Band 2 Haralick Sum Average 200 m mean
	B02_hara_SA_200m_sd	Sentinel Band 2 Haralick Sum Average 200 m standard deviation
	B02_hara_SE 0.0205	Sentinel Band 2 Haralick Sum Entropy
	B02_hara_SE_200m_mean	Sentinel Band 2 Haralick Sum Entropy 200 m mean
	B02_hara_SE_200m_sd	Sentinel Band 2 Haralick Sum Entropy 200 m standard deviation
	B02_hara_SV 0e+00	Sentinel Band 2 Haralick Sum Variance
	B02_hara_SV_200m_mean	Sentinel Band 2 Haralick Sum Variance 200 m mean
	B02_hara_SV_200m_sd	Sentinel Band 2 Haralick Sum Variance 200 m standard deviation
	B02_hara_Var 0.0011	Sentinel Band 2 Haralick Variance
	B02_hara_Var_200m_mean	Sentinel Band 2 Haralick Variance 200 m mean
	B02_hara_Var_200m_sd	Sentinel Band 2 Haralick Variance 200 m standard deviation